Polymer 143 (2018) 258–270

Contents lists available at ScienceDirect

Polymer

journal homepage: www.elsevier.com/locate/polymer

Sequence length distribution affects the lower critical solution temperature, glass transition temperature, and CO_2-responsiveness of *N*-isopropylacrylamide/methacrylic acid copolymers

Yeong-Tarng Shieh [a, *], Pei-Yi Lin [a, b], Shiao-Wei Kuo [b, c, **]

[a] Department of Chemical and Materials Engineering, National University of Kaohsiung, Kaohsiung, Taiwan, ROC
[b] Department of Materials and Optoelectronic Science, National Sun Yat-Sen University, Kaohsiung, Taiwan, ROC
[c] Department of Medicinal and Applied Chemistry, Kaohsiung Medical University, Kaohsiung, Taiwan, ROC

ARTICLE INFO

Article history:
Received 12 October 2017
Received in revised form
6 March 2018
Accepted 1 April 2018
Available online 10 April 2018

Keywords:
Sequence length distribution
Hydrogen bonding
LCST
CO_2-Responsiveness

ABSTRACT

In this study we investigated the effects of the sequence length distributions in random and block copolymers of *N*-isopropylacrylamide and methacrylic acid (MAA)—PNIPAm-*co*-PMAA and PNIPAm-*b*-PMAA, prepared through free radical copolymerization and reversible addition fragmentation chain transfer (RAFT) polymerization, respectively—on their lower critical solution temperature (LCST), glass transition temperatures (T_g), and CO_2-responsiveness. The insertion of the PMAA segment into PNIPAm enhanced the thermal properties (e.g., higher values of T_g) because of strong hydrogen bonding between the carboxylic acid units of the PMAA segment and the amide units of the PNIPAm segment, as determined using Fourier transform infrared and ^{1}H NMR spectroscopy. The LCST increased upon increasing the pH for both the random and block copolymers, because the COOH units of the PMAA segments dissociated to form COO^- groups, which improved the solubility in aqueous solutions. Furthermore, the variation in the LCST of PNIPAm93-b-PMAA7 with respect to pH was greater than that of PNIPAm-*co*-PMAA, due to the sequence length distribution effect. Treatment with supercritical CO_2 ($scCO_2$) also caused the values of T_g to increase for PNIPAm-*co*-PMAA but decrease for PNIPAm93-b-PMAA7, presumably because CO_2 in the micelle structure of the block copolymer had a plasticization effect. Reversible CO_2-responsiveness of the block copolymer in aqueous solution was evidenced by the appearance and disappearance of cloudy aqueous solutions upon alternating bubbling with CO_2 and N_2; this behavior was not observed for the random copolymers.

1. Introduction

Hydrogen bonding in polymer materials has received much attention for its ability to improve the miscibility of polymer blends [1–4], change a variety of physical properties (e.g., thermal, mechanical, surface, and rheological properties) [5–8], favor the self-assembly of supramolecular nanostructures [9–12], and facilitate the preparation of polymer nanocomposites [13–15]. The hydrogen bonding strength in polymer blends and copolymers is strongly dependent on the affinity between the hydrogen bonding donor and acceptor units [16–18]. In addition, the hydrogen bonding strength in hydrogen-bonded copolymers is always higher than that in hydrogen-bonded polymer blend systems because of the different degrees of rotational freedom from intramolecular screening and functional group accessibility effects; such behavior has been observed, for example, in blends of polyvinylphenol (PVPh) with poly (ethyl methacrylate) (PEMA) and poly (4-vinylpyridine) (P4VP), as well as many other hydrogen-bonded blend and copolymer systems [19–22].

Smart polymers are materials that undergo variations in their physical properties (e.g., swell or shrink) upon small changes in their environment (e.g., temperature, pH, or ionic strength) [23–25]. poly (*N*-isopropylacrylamide) (PNIPAm) is the benchmark responsive polymer material; it has a lower critical solution temperature (LCST) of approximately 32 °C, where it undergoes a sharp coil-to-globule transition in aqueous solution from a hydrophilic to a hydrophobic

* Corresponding author.
** Corresponding author. Department of Materials and Optoelectronic Science, National Sun Yat-Sen University, Kaohsiung, Taiwan, ROC.
E-mail addresses: yts@nuk.edu.tw (Y.-T. Shieh), kuosw@faculty.nsysu.edu.tw (S.-W. Kuo).

https://doi.org/10.1016/j.polymer.2018.04.002
0032-3861/

state above the LCST [26,27]. In addition, polymer materials featuring acrylic acid segments can also undergo the same coil-to-globule transition in aqueous solution upon varying the pH—a characteristic that has been exploited for drug-delivery applications [28–30]. Because carbonyl (C=O) units are present in both NIPAm and acrylic acid monomers, they can interact with carbon dioxide (CO_2) through dipole–dipole interactions [31–33]. As a result, random copolymers incorporating both acrylic acid and NIPAm units can display temperature, pH, and CO_2 stimuli-responsive behavior in aqueous solution [34–36]. For example, in a previous study we synthesized a series of poly (*N*-isopropylacrylamide-*co*-acrylic acid) (PNIPAm-*co*-PAA) copolymers through free radical copolymerization and investigated their hydrogen bonding interactions, LCST behavior, and thermal properties under a CO_2 atmosphere [37].

We are unaware, however, of any previous investigations into the effects of the sequence length distribution and corresponding strength of hydrogen bonding between the PNIPAm and acrylic acid segments on the temperature, pH, and CO_2 stimuli-responsive behavior of their copolymers in aqueous solution. In this study, we chose methacrylic acid (MAA) as the pH-responsive unit because the presence of MAA units in a polymer main chain results in thermal properties and greater hydrophobicity superior to those for acrylic acid (AA) units, while also allowing greater stimuli-responsiveness in aqueous solution. Accordingly, we prepared PNIPAm-*b*-PMAA diblock copolymers through sequential reversible-addition/fragmentation chain transfer (RAFT) radical polymerization of *tert*-butyl methacrylate with NIPAm monomer and selective hydrolysis of the *tert*-butyl groups, and corresponding PNIPAm-*co*-PMAA random copolymers through direct free radical copolymerization (Scheme 1).

We then used differential scanning calorimetry (DSC), Fourier transform infrared (FTIR) spectroscopy, nuclear magnetic resonance (NMR) spectroscopy, and UV–Vis spectroscopy to examine the compositions, thermal properties, strength of hydrogen bonding, LCST behavior, and CO_2 responsiveness of these two copolymers featuring different sequence length distributions.

2. Experimental

2.1. Materials

N-Isopropylacrylamide (NIPAm, Tokyo Kasei) was recrystallized from hexane. Methacrylic acid (MAA, Alfa Aesar) and *tert*-butyl methacrylate (tBMA, Tokyo Chemical Industry) were distilled under reduced pressure. Azobis (isobutyronitrile) (AIBN, Aldrich) was recrystallized from methanol. 2-(2-Cyano-2-propyl)-*S*-dodecyltrithiocarbonate (CPDT, Strem Chemicals) was used as received. Dioxane (J. T. Baker) was distilled prior to use. All other solvents were obtained in the highest purity available and used as received.

2.2. Free radical copolymerizations of PNIPAm-co-PMAA random copolymers

The monomers NIPAm and MAA (various ratios, 2 M monomer mixture) and the initiator AIBN (0.05 M) were stirred in MeOH under N_2 to obtain a homogeneous solution that was heated in a circulated thermostat oil bath at 55 °C for 4 h. To purify the pure PNIPAm homopolymer, the homopolymer was first dissolved in MeOH (80 mL) at 25 °C and then poured into deionized water (100 mL) at 45 °C to precipitate the product. After removing the clear supernatant, the precipitate was again dissolved in MeOH (80 mL) and reprecipitated from deionized water (100 mL) of 45 °C. This dissolution/precipitation procedure was repeated a third time, followed by vacuum drying at 60 °C for 24 h, to give the pure PNIPAm homopolymer. To purify the PMAA homopolymer, the reaction mixture was concentrated and then ether (200 mL) was added to form a precipitate, which was subjected to vacuum drying for 24 h. To purify the PNIPAm-*co*-PMAA random copolymer, the copolymer was dissolved in MeOH (50 mL) at 25 °C and then ether (200 mL) was added to form a precipitate. The filtrate was then treated with concentrated HCl (a few drops) and heated at 60 °C to give the PNIPAm-*co*-PMAA random copolymer as a precipitate, which was washed with ether until neutral, followed by vacuum

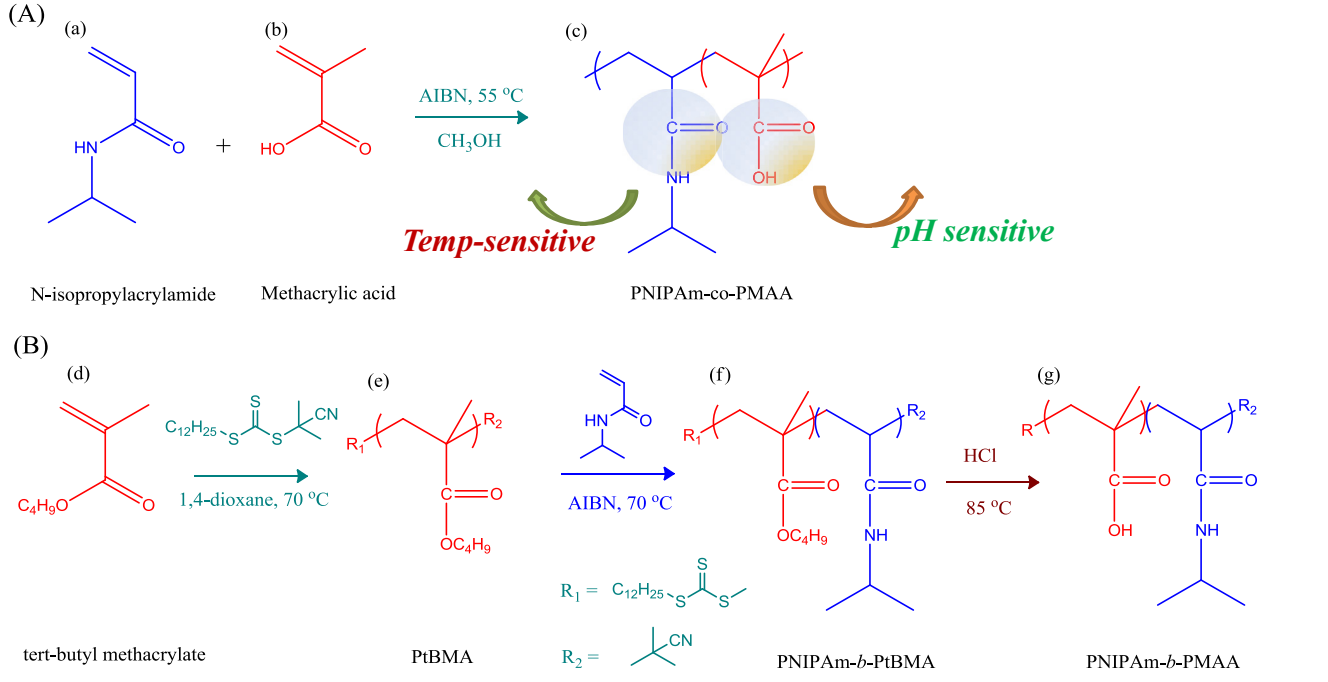

Scheme 1. (A) Synthesis of PNIPAm-*co*-PMAA random copolymers (c) from random copolymerization of the monomers (a) *N*-isopropylacrylamide and (b) methacrylic acid. (B) Synthesis of PNIPAm-*b*-PMAA block copolymer (g) from RAFT polymerization of (d) *tert*-butyl methacrylate monomer, (e) PtBMA homopolymer, and (f) PNIPAm-*b*-PtBMA block copolymer.

drying for 24 h.

2.3. RAFT polymerization of PNIPAm-b-PMAA diblock copolymer

A solution of tBMA, CPDT, and AIBN (molar concentration ratio: 2240:10:1) in 1,4-dioxane (12 mL) in a reaction vessel was degassed through three freeze/pump/thaw cycles, sealed under vacuum, and placed in a thermostat oil bath (70 °C) for 48 h. The reaction product was precipitated in water/MeOH (1:4, 250 mL), filtered, and dried under vacuum to give the tBMA homopolymer (PtBMA). PtBMA, used as a RAFT macroinitiator, was dissolved in 1,4-dioxane (30 mL) and then NIPAm (8 g) and AIBN (20 mg) were added to the reaction vessel; the mixture was degassed through three freeze/pump/thaw cycles, sealed under vacuum, and placed in a thermostat oil bath (70 °C) for 48 h. The reaction product was precipitated in water/MeOH (1:1, 400 mL), filtered, and dried under vacuum for 24 h, to give the PtBMA-*b*-PNIPAm block copolymer. Hydrolysis of the tBMA block segment of the copolymer was conducted in the presence of aqueous hydrochloric acid (1 mL) in 1,4-dioxane (30 mL) at 85 °C for 24 h. The resulting solution was dried (Na_2SO_4) and filtered. The filtrate was treated with ether (200 mL) to give a precipitate, which was dried under vacuum for 24 h to give the PNIPAm-*b*-PMAA copolymer.

2.4. Characterization

A Bruker Tensor-27 FTIR spectrometer was used (conventional KBr disk method) to record FTIR spectra of the copolymers. The spectra were measured at room temperature with a resolution of 4 cm^{-1} and a sensitivity of 32 scans. The molecular weights and polydispersity (PDI) indices of the synthesized copolymers were determined using a Waters 510 gel permeation chromatography (GPC) system equipped with a refractive index detector. Dimethylformamide (DMF) was used as the eluent at a flow rate of 0.8 mL min^{-1} at 25 °C. ^{1}H NMR spectra of polymer solutions in deuterated dimethylsulfoxide (DMSO-d_6) were recorded using a Varian Unity Inova-500 MHz spectrometer. The LCSTs of the copolymers (5 wt% aqueous solutions) were determined at various values of pH by measuring their visible light transmittance at 550 nm with respect to temperature (from high to low temperature during measurements). Herein, we determined the LCST behavior from high to low temperature because this was easier to do and took no need of heating. In addition, during the measurement, we very slowly cooled the aqueous solution sample to equilibrate at a temperature to record the transmittance [38]. The inflection point of the transmittance–temperature curve was assigned as the LCST of the copolymer aqueous solution. Glass transition temperatures (T_g) of copolymers, cast from aqueous solutions at various values of pH, were measured through differential scanning calorimetry (DSC), with a first heating and cooling cycle at 20 °C/min between 40 and 200 °C followed by heating at 10 °C/min to 200 °C to record the value of T_g. The CO_2-dependence of the values of T_g of cast films of various copolymer compositions was also investigated after treatment in supercritical carbon dioxide ($scCO_2$) fluid at 2000 psi and 32 °C for 1 h and subsequent depressurization for 1 h.

3. Results and discussion

3.1. Synthesis of PNIPAm-co-PMAA random copolymers

We synthesized various PNIPAm-*co*-PMAA random copolymers through free radical copolymerization, as displayed in Scheme 1(A), and then used FTIR and NMR spectroscopy to calculate the copolymer compositions. The reason why we synthesized the random copolymers through free radical copolymerization was because it took much less time and was easy to carry out. In this study, we aimed to investigate the sequence length distribution effects on the LCST, T_g, and CO_2 responsiveness of the copolymers. The general free radical copolymerization could provide copolymers with random sequence length distribution for the comparison with block copolymers. Fig. 1(A) presents the ^{1}H NMR spectra of the PNIPAm-*co*-PMAA random copolymers. The signals for the C**H**$_2$ and C**H** protons of the main chain of pure PNIPAm appeared at 1.96 and 1.46 ppm, while the signals for the other C**H**$_3$ and C**H** protons appeared as multiplets at 1.02 and 3.86 ppm; more importantly, the signal for the amide proton (CON**H**) appeared at 7.21 ppm as a singlet [Fig. 1(A)–(a)]. Similarly, the signals for the C**H**$_3$ and C**H**$_2$ protons of the main chain of pure PMAA appeared between 0.91 and 1.76 ppm, with the signal for the carboxylic acid proton (COO**H**) appearing at 12.30 ppm as a singlet [Fig. 1(A)–(g)]. As a result, we could calculate the copolymer compositions of the PMAA segments from the peak intensity ratio, $\boldsymbol{A}_{COOH}/(\boldsymbol{A}_{COOH} + \boldsymbol{A}_{CONH})$, based on the signals at 12.30 and 7.21 ppm. Similarly, we could also determine this ratio using FTIR spectroscopy [Fig. 1(B)]: the spectrum of pure PNIPAm featured two major peaks for the amide I and amide II absorptions at 1644 and 1544 cm^{-1}, respectively, while that for pure PMAA exhibited a signal for self-associated hydrogen-bonded carboxylic acid dimers at 1702 cm^{-1}. The peak ratio of $\boldsymbol{A}_{COOH}/(\boldsymbol{A}_{COOH} + \boldsymbol{A}_{CONH})$ increased upon increasing the PMAA content in the PNIPAm-*co*-PMAA random copolymers. Table 1 summarizes the feed ratios and resultant PNIPAm-*co*-PMAA random copolymer compositions calculated from the ^{1}H NMR spectroscopic analyses. We could calculate the reactivity ratios of these two monomers based on the Kelen–Tudos plot, as we have described previously [39,40]. Fig. 2 displays the calculated values of r_{PNIPAm} and r_{PMAA} of 0.72 and 1.12, respectively, implying that PNIPAm-*co*-PMAA formed random to ideal copolymers.

3.2. Synthesis of PNIPAm-b-PMAA diblock copolymers

We used sequential RAFT polymerization to prepare the PNIPAm93-*b*-PMAA7 diblock copolymer [Scheme 1(B)]. We first prepared a PtBMA homopolymer and then used it as a RAFT macroinitiator to synthesize a PNIPAm-*b*-PtBMA diblock copolymer through sequential RAFT polymerization. Finally, we selectively hydrolyzed the *tert*-butyl ester units to form a PNIPAm-*b*-PMAA diblock copolymer, the structure of which was confirmed using ^{1}H NMR and FTIR spectroscopy (Fig. 3).

Fig. 3(B)-(a) reveals that the signal for the C=O groups appeared at 1724 cm^{-1} for the pure PtBMA homopolymer, with the signal for the amide I absorption appearing at 1652 cm^{-1} for the PNIPAm-*b*-PtBMA diblock copolymer. After selective hydrolysis of the *tert*-butyl ester groups to form the PNIPAm93-b-PMAA7 diblock copolymer, we observed a broad signal between 2500 and 3500 cm^{-1} for the COOH units, with the amide I absorption shifted slightly to 1645 cm^{-1}, implying the presence of hydrogen bonds between the carboxylic acid units of the PMAA block and the amide units of the PNIPAm block. Again, we determined the composition of the PMAA copolymer from the peak ratio $\boldsymbol{A}_{COOH}/(\boldsymbol{A}_{COOH} + \boldsymbol{A}_{CONH})$, based on the signals 12.00 and 7.21 ppm [Fig. 3(A)]. Table 2 summarizes the molecular weight and block copolymer composition of this PNIPAm93-b-PMAA7 block copolymer. Herein, we need to emphasize that it is difficult to accurately determine molecular weights of PNIPAm and its copolymer by GPC analysis because strong intramolecular and intermolecular interactions are present in these polymers and affect the hydrodynamic volume of polymer sample and thus the GPC results. These intramolecular and intermolecular interactions, however, do not affect the determination of the sequence length distribution in both random and block copolymers in this study.

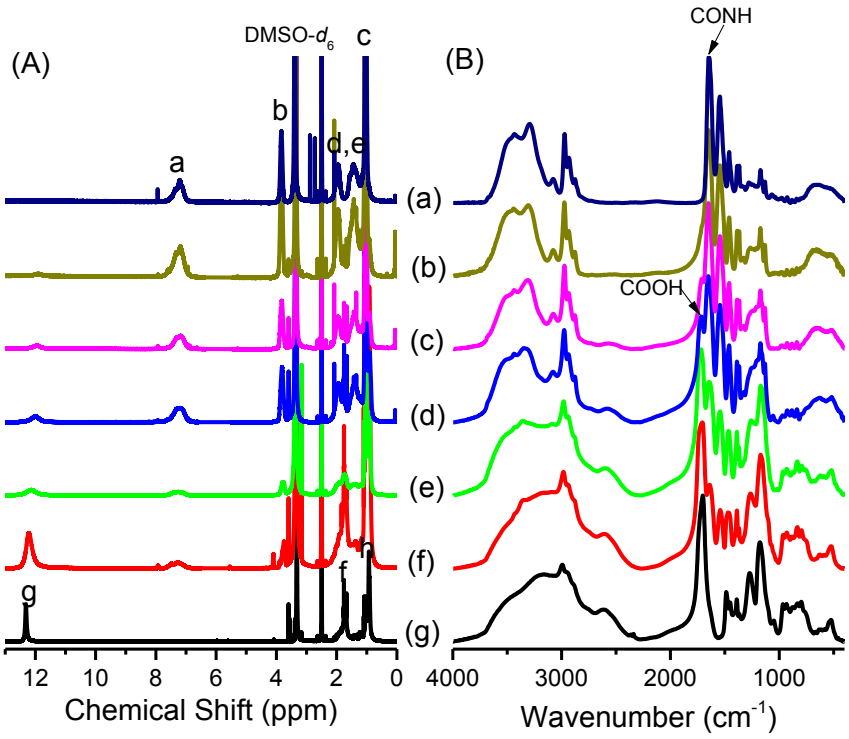

Fig. 1. (A) ^{1}H NMR and (B) FTIR spectra of (a) pure PNIPAm; (b) PNIPAm93-*co*-PMAA7; (c) PNIPAm79-*co*-PMAA21; (d) PNIPAm74-*co*-PMAA26; (e) PNIPAm40-*co*-PMAA60; (f) PNIPAm22-*co*-PMAA78, and (g) pure PMAA.

Table 1
Characteristics of PNIPAm-*co*-PMAA copolymers used in this study.

Abbreviation	Monomer feed (mol %)		Polymer composition (mol %)		T_g (°C)	M_n (g/mol)	PDI
	NIPAm	MAA	NIPAm	MAA			
PNIPAm	100	0	100	0	140.6	3.1×10^4	1.64
PNIPAm93-*co*-PMAA7	95	5	93.2	6.8	141.3	1.0×10^5	1.52
PNIPAm79-*co*-PMAA21	85	15	79.3	20.7	166.3	3.5×10^4	1.19
PNIPAm74-*co*-PMAA26	75	25	74.2	25.8	172.6	9.9×10^3	1.24
PNIPAm40-*co*-PMAA60	50	50	40.1	59.9	181.4	3.8×10^5	1.57
PNIPAm22-*co*-PMAA78	25	75	22.5	77.5	179.5	4.5×10^5	1.58
PMAA	0	100	0	100	177.5	1.3×10^5	1.19

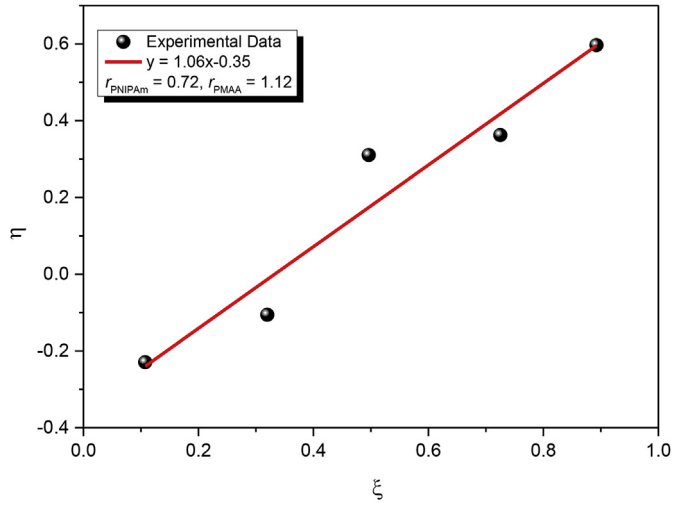

Fig. 2. Kelen–Tudos plot for determination of the reactivity ratios for PNIPAm-*co*-PMAA random copolymers.

3.3. Thermal properties of PNIPAm-co-PMAA copolymers

Fig. 4(A) presents the second-run DSC thermograms, recorded over the range from 50 to 200 °C, of the pure PMAA, the pure PNIPAm, and a series of PNIPAm-*co*-PMAA random copolymers. The pure PMAA and pure PNIPAm displayed values of T_g of approximately 178 and 140 °C, respectively, with all the random PNIPAm-*co*-PMAA copolymers exhibiting only single-T_g behavior in the range 141–181 °C. The Kwei equation can be used to predict the behavior of the values of T_g for hydrogen-bonded blends and copolymer systems [41]:

$$T_g = \frac{W_1 T_{g1} + kW_2 T_{g2}}{W_1 + kW_2} + qW_1 W_2 \quad (1)$$

where W_i and T_{gi} correspond to the weight fraction and glass transition temperature of each polymer.

Segment, respectively, and k and q are fitting constants reflecting the strength of the hydrogen bonding interactions. We obtained values of k and q of 1 and 100, respectively, based on the Kwei

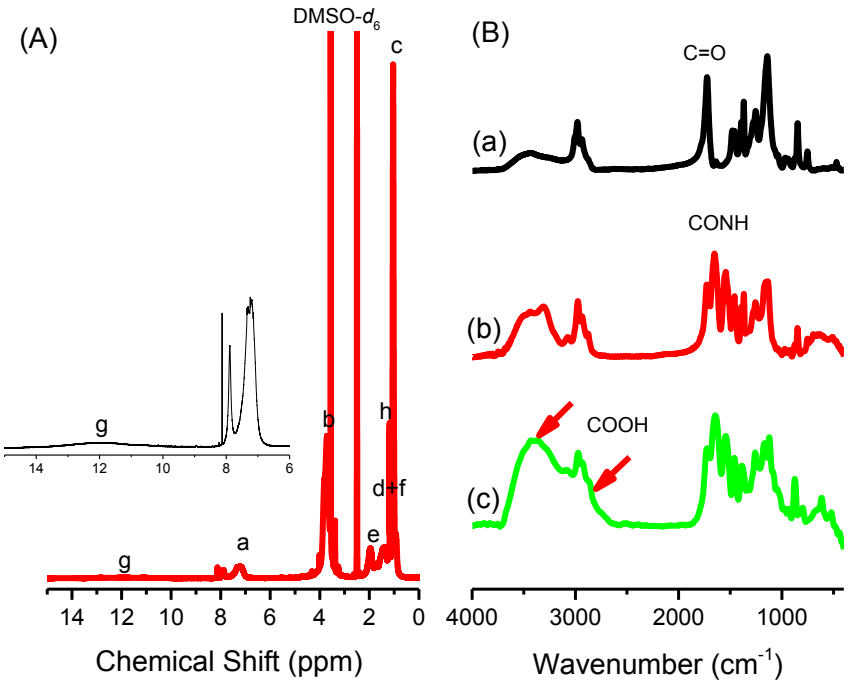

Fig. 3. (A) ^{1}H NMR spectra of PNIPAm-*b*-PMAA and (B) FTIR spectra of (a) pure PtBMA, (b) PNIPAm-*b*-PtBMA, and (c) PNIPAm-*b*-PMAA block copolymer.

Table 2
Characterization data for the PtBMA, PNIPAm-*b*-PtBMA, and PNIPAm-*b*-PMAA block copolymers used in this study.

	M_n (g/mol)	M_w (g/mol)	PDI
PtBMA	6300	7200	1.15
PNIPAm-*b*-PtBMA	9.4×10^4	1.3×10^5	1.25
PNIPAm93-b-PMAA7	5.9×10^4	7.5×10^4	1.42

equation (green line), as displayed in Fig. 4(B). The positive value of q (higher than the linear rule, blue line) implies that the intermolecular hydrogen bonding in the random copolymer PNIPAm-*co*-PMAA [Scheme 2(c)] was stronger than the self-association hydrogen bonding of the PMAA [Scheme 2(a)] and PNIPAm [Scheme 2(b)] segments.

Fig. 5 displays the second-run DSC thermograms of the pure PMAA, the pure PNIPAm, and the PNIPAm93-b-PMAA7 block copolymer synthesized in this study. Similarly, the block copolymer

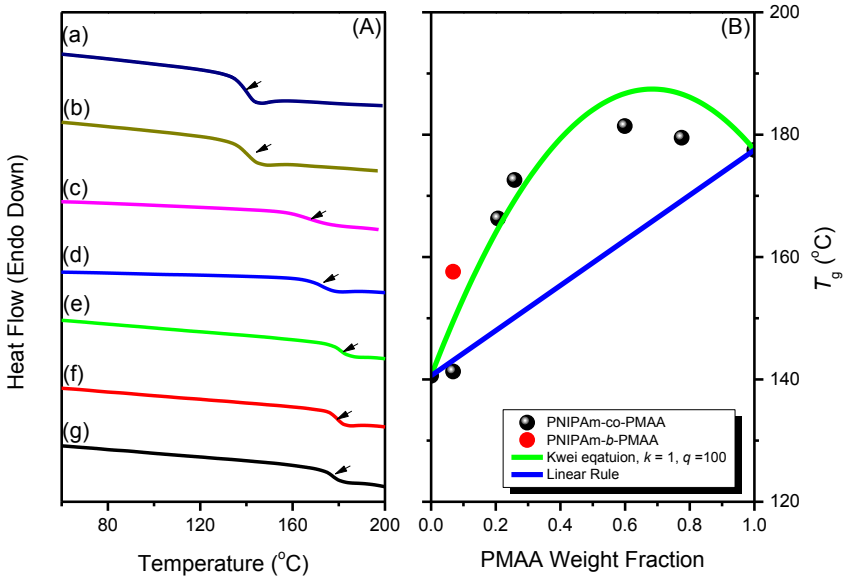

Fig. 4. (A) DSC thermograms of PNIPAm-*co*-PMAA random copolymers: (a) pure PNIPAm; (b) PNIPAm93-*co*-PMAA7; (c) PNIPAm79-*co*-PMAA21; (d) PNIPAm74-*co*-PMAA26; (e) PNIPAm40-*co*-PMAA60; (f) PNIPAm22-*co*-PMAA78, and (g) pure PMAA. (B) Experimental values of T_g for the random copolymers (black spheres) and block copolymer (red spheres), with lines predicted by the Kwei (green line) and linear (blue line) equations. (For interpretation of the references to colour in this figure legend, the reader is referred to the Web version of this article.)

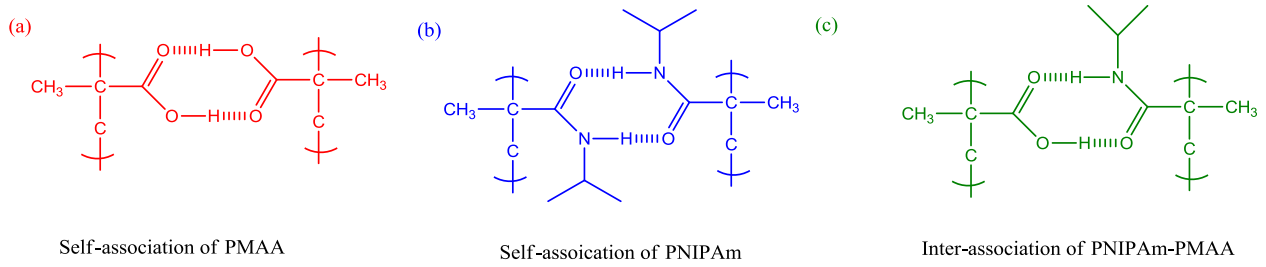

Scheme 2. The possible self-association and inter-association of PNIPAm-*co*-PMAA copolymers: (a) self-association of PMAA segment, (b) self-association of PNIPAm segment, and (c) inter-association of PNIPAm-*co*-PMAA copolymers.

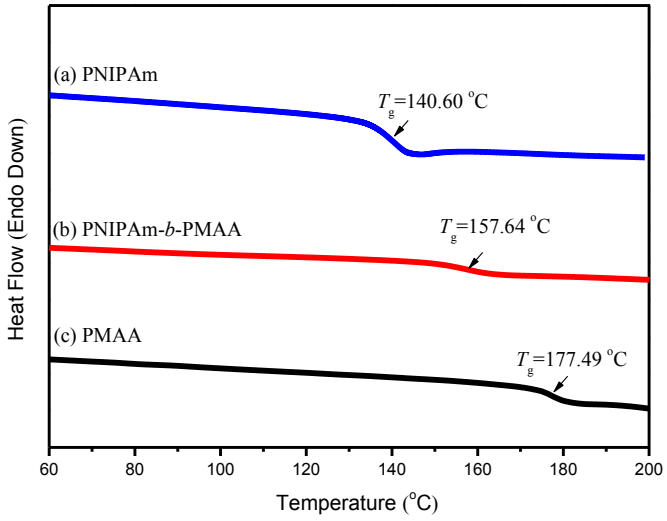

Fig. 5. DSC thermograms of (a) pure PNIPAm, (b) PNIPAm93-b-PMAA7, and (C) PMAA homopolymer.

of.

PNIPAm93-b-PMAA7 also exhibited single-T_g behavior at 157 °C; in comparison, immiscible diblock copolymers usually exhibit two values of T_g behavior. Therefore, we concluded that the miscible PNIPAm93-b-PMAA7 block copolymer also featured strong intermolecular hydrogen bonding; indeed, its value of T_g was higher than that of the random copolymer PNIPAm-*co*-PMAA at a similar weight fraction [Fig. 4(B) (red point)]. We used FTIR and NMR spectroscopy to investigate the intermolecular hydrogen bonding in these two different types of copolymer sequences. Fig. 6(A) displays ^{1}H NMR spectra of the PNIPAm-*co*-PMAA random copolymers. We observed an upfield shifts of the signal for the proton of the COOH units of the PMAA segment upon increasing the PNIPAm content in the PNIPAm-*co*-PMAA random copolymer in D_2O solution: from 12.30 ppm for the pure PMAA to 11.90 ppm for PNIPAm93-*co*-PMAA7. In addition, the signal of the proton of the COOH groups also shifted upfield (to 12.00 ppm) for the PNIPAm93-b-PMAA7 block copolymer, suggesting the existence of intermolecular hydrogen bonding between the COOH and CONH units in both the PNIPAm-*co*-PMAA random copolymers and the PNIPAm93-*b*-PMAA7 block copolymer [Scheme 2(c)].

Fig. 6(B) displays the C═O region in the FTIR spectra of PNIPAm-

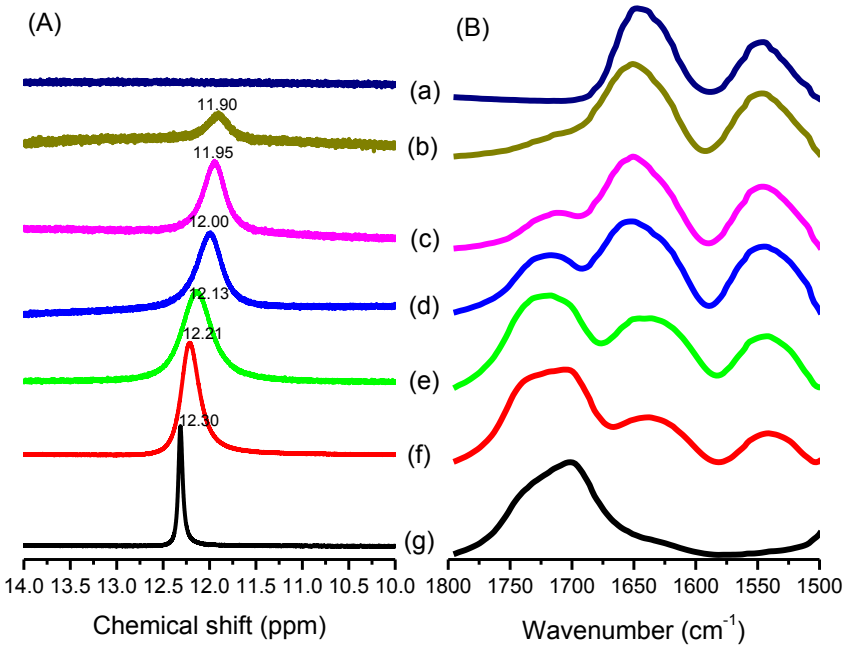

Fig. 6. (A) ^{1}H NMR spectra, presented in the range 14–10 ppm, displaying the signal of the proton of the acrylic acid units. (B) FTIR spectra, in the range 1800–1500 cm^{-1}, displaying the COOH and CONH absorptions of (a) pure PNIPAm; (b) PNIPAm93-*co*-PMAA7; (c) PNIPAm79-*co*-PMAA21; (d) PNIPAm74-*co*-PMAA26; (e) PNIPAm40-*co*-PMAA60; (f) PNIPAm22-*co*-PMAA78, and (g) pure PMAA.

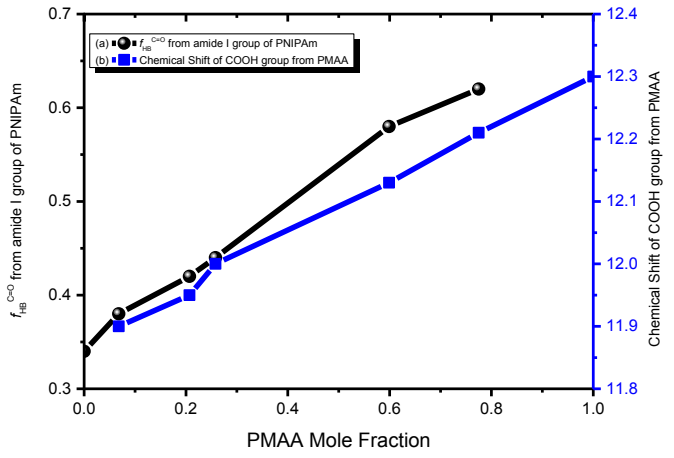

Fig. 7. Fractions of hydrogen-bonded amide I units of PNIPAm segment and chemical shift of COOH groups in PMAA for various PMAA molar fractions.

co-PMAA random copolymers. As mentioned in our discussion of Fig. 1(B), the spectrum of the pure PNIPAm featured two major peaks for amide I and amide II absorptions at 1644 and 1544 cm^{-1}, respectively, while the spectrum of the pure PMAA exhibited a signal for the self-associated hydrogen bonded carboxylic acid dimer at 1702 cm^{-1}. The signal of the amide I group of PNIPAm split into two absorption bands upon increasing the PMAA content in the random copolymers PNIPAm-*co*-PMAA—one signal corresponding to inter-molecularly hydrogen bonded amide groups at 1615 cm^{-1} and the other for free amide I groups at 1644 cm^{-1}; these two bands were fit well by the Gaussian function.

Fig. 7 summarizes the fraction of hydrogen-bonded amide groups of the PNIPAm segment and the chemical shift of the COOH protons of the PMAA segment. The fraction of hydrogen-bonded amide I groups of the PNIPAm segment increased upon increasing the PMAA content in the PNIPAm-*co*-PMAA random copolymers. The signal for the COOH protons of the PMAA segment shifted upfield upon increasing the PNIPAm content in the PNIPAm-*co*-PMAA random copolymers, as expected. All these results are consistent with strong intermolecular hydrogen bonding between the COOH and CONH units that improved the thermal properties, based on DSC analyses.

3.4. LCST behavior of PNIPAm-co-PMAA random copolymers

PNIPAm random coils in aqueous solution generally collapse to form dense globular chains at a temperature of approximately 32 °C. We suspected that our PNIPAm-*co*-PMAA copolymers would display both temperature- and pH-responsive behavior in aqueous solution. Herein, we need to emphasize that although the PNIPAm-*co*-PMAA random copolymer and PNIPAm-*b*-PMAA block copolymer were prepared through different methods, we focus on the investigation of the effects of sequence length distribution in random and block copolymers on their LCST, T_g, and CO_2 responsiveness in this study. Fig. 8 presents UV spectra of the PNIPAm-*co*-PMAA copolymers, revealing how the transparent copolymer solution became opaque when the temperature was higher than a specific value at a pH. The opaque solution reformed a transparent solution when the temperature decreased, revealing reversible phase transition behavior.

Furthermore, the LCST increased upon increasing the pH for all of the PNIPAm-*co*-PMAA random and block copolymers (Fig. 8), implying greater solubility at higher values of pH in aqueous solution; Fig. 9 summarizes the LCSTs. Because the COOH units of the PMAA segment dissociated into COO^- groups to greater degrees upon increasing the pH, the solubility improved accordingly in the aqueous solution, thereby enhancing the LCST. In addition, the LCSTs were affected significantly upon increasing the PMAA

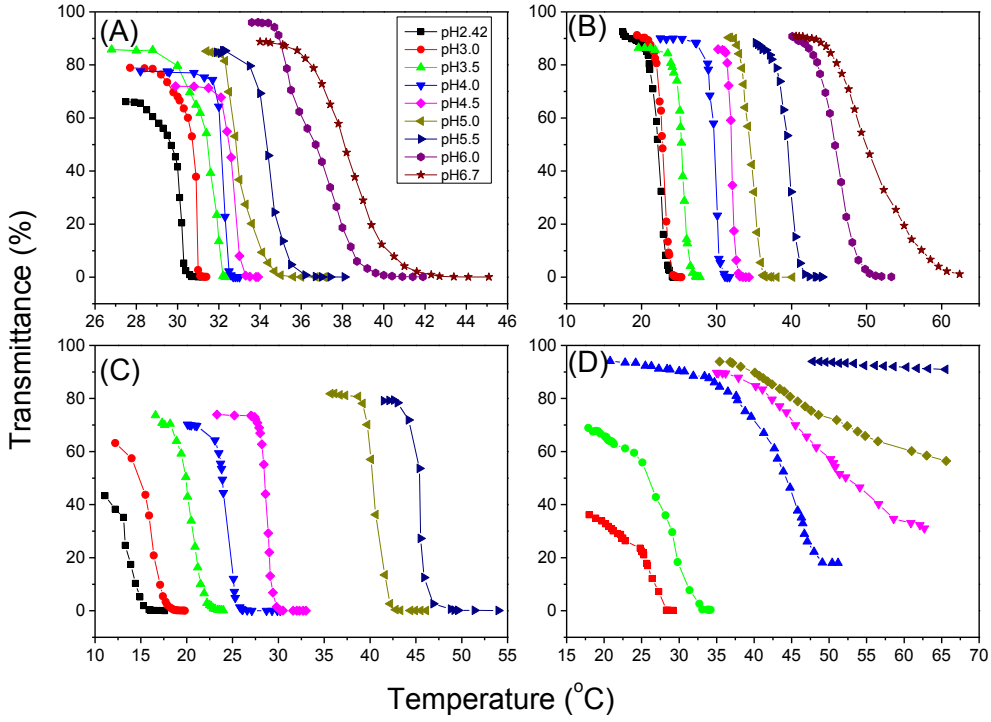

Fig. 8. Transmittance (from UV–Vis spectra) of aqueous solutions at various temperatures and values of pH at 550 nm for (A) PNIPAm93-*co*-PMAA7, (B) PNIPAm79-*co*-PMAA21, and (C) PNIPAm74-*co*-PMAA26, and (D) the PNIPAm93-b-PMAA7 block copolymer.

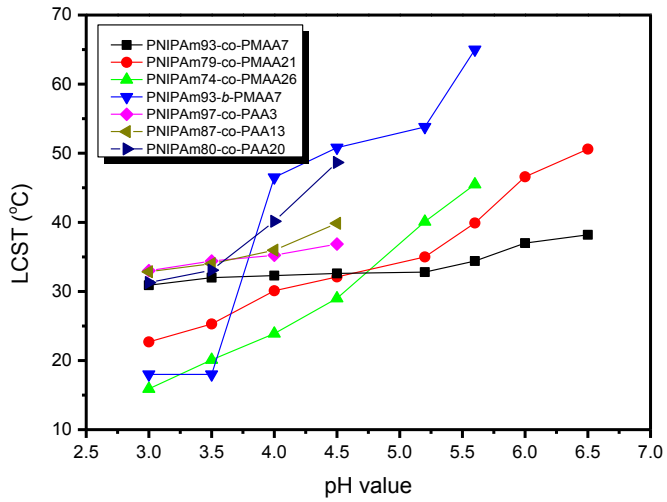

Fig. 9. Corresponding LCSTs of aqueous solutions of PNIPAm-*co*-PMAA, PNIPAm93-b-PMAA7, and PNIPAm-*co*-PAA copolymers at various values of pH.

content in the random copolymers. For example, the LCST for the random copolymer PNIPAm93-*co*-PMAA7 increased slightly from 30.9 °C at pH 3.0–38.2 °C at pH 6.7, whereas for PNIPAm74-*co*-PMAA26 it increased dramatically from 15.9 °C at pH 3.0–42.5 °C at pH 6.7, suggesting that the PMAA content in the PNIPAm-*co*-PMAA random copolymers did indeed influence the LCST behavior in response to the pH. In addition, higher PMAA contents in PNIPAm-*co*-PMAA random copolymers led to lower LCSTs (Fig. 9) because the higher PMAA content resulted in a higher fraction of intermolecular hydrogen bonding interactions between the PNIPAm and PMAA segments (Fig. 7), thereby inhibiting the inter-association of the amide groups of PNIPAm and H_2O molecules; accordingly, these random copolymers became more hydrophobic in the aqueous solution and exhibited lower LCSTs [41]. The COOH units of the PMAA segment would also dissociate into the COO^- groups at higher values of pH; thus, higher PMAA contents in the random copolymers improved the hydrophilicity and solubility behavior in the H_2O solution and, thus, induced higher LCSTs. Here we should mention that PMAA segment or block at pH of higher than 6.7 was water-soluble over wide temperature range and caused disappearance of LCST for its copolymers in this study. This was why we did not present the LCST data above pH 6.7.

Compared with the PNIPAm-*co*-PAA random copolymers, the presence of methyl groups in the PMAA segment led to copolymers that were more hydrophobic in H_2O solution, thereby inducing LCSTs lower than those of copolymers featuring PAA segments at lower values of pH (pH < 4.5), as revealed in Fig. 9. Because of the improved hydrophilicity and solubility in H_2O for the PNIPAm-*co*-PAA random copolymers, we did not observe the LCST behavior when the pH was greater than 4.5. We did, however, observe that the PNIPAm-*co*-PMAA random copolymer exhibited LCST behavior when the pH was between 4.5 and 6.7, because the ability of the COOH units of the PMAA segment to dissociate into COO^- groups at higher pH was lower than that of the PAA segment in H_2O. Similarly, the PNIPAm93-b-PMAA7 block copolymer exhibited lower LCST behavior at lower values of pH, and higher LCST behavior at higher values of pH. At lower values of pH, the PNIAAm93-b-PMAA7 block copolymer may have formed a micelle structure [Scheme 3(b)], with the PMAA block as the core and the PNIPAm block as the corona, because of the poor solubility of the PMAA block segment. As a result, the block copolymer would become more hydrophobic in aqueous solution and, thereby, induce a lower LCST [42–44]. At higher values of pH, the COOH groups of the PMAA block segment would undergo dissociation into COO^- groups in a manner superior to that of in random copolymers, because the MAA segments randomly inserted into the NIPAm segments in the random copolymer would induce stronger inter-association of the PNIPAm and PMAA segments through an intra-molecular screening effect and, thereby, minimize inter-association with H_2O (thus, a decrease in the LCST for the random copolymer). As a result, the block copolymer might have superior hydrophilicity and solubility in H_2O and, thereby, induce higher LCSTs relative to

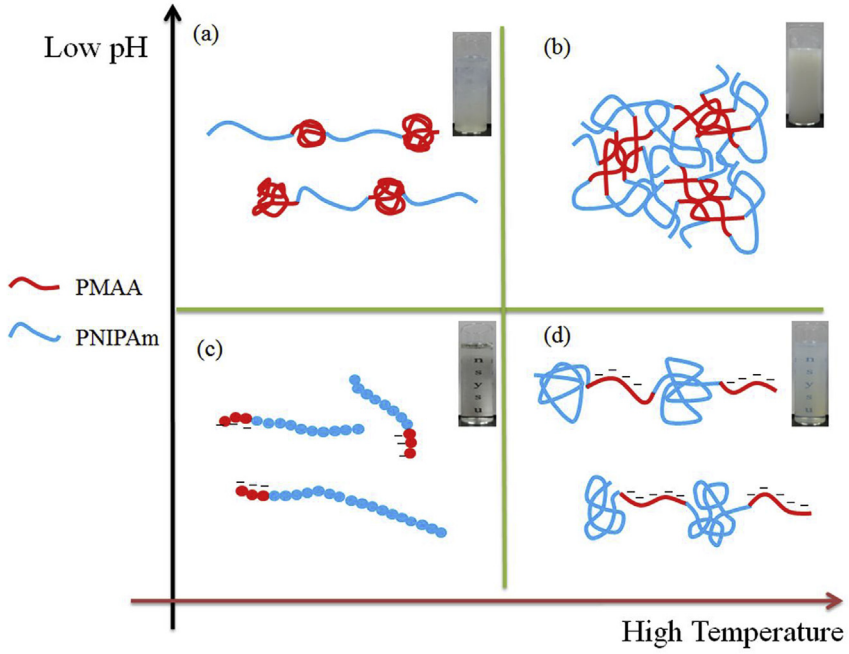

Scheme 3. Possible chain behavior of the PNIPAm93-b-PMAA7 diblock copolymer in aqueous solutions at various values of pH and temperature.

those of the random copolymer. Fig. 10 provides photographs of the 3 wt% PNIPAm93-b-PMAA7 block copolymer and summarizes all of its possible chain behavior (Scheme 3) at different values of pH and temperature.

3.5. Thermal properties of PNIPAm-co-PMAA random copolymers under CO_2 atmosphere

Fig. 11 summarizes the DSC thermograms, recorded in the range from 60 to 200 °C, of thin films of the various PNIPAm-*co*-PMAA random copolymers and PNIPAm93-*b*-PMAA7 block copolymer after treatment at various values of pH.

At relatively lower values of pH, all of the PNIPAm-*co*-PMAA random and block copolymers exhibited relatively high glass transition temperatures. The values of T_g decreased at lower values of pH and then increased at relatively higher values of pH. The lower values of pH presumably led to greater degrees of inter-association between the PNIPAm and PMAA segments, thereby leading to higher values of T_g. Upon increasing the pH, some of the COOH groups in the PMAA segment would dissociate into COO^- groups, thereby inhibiting the inter-association of the PNIPAm and PMAA units; the negatively charged COO^- groups would induce strong repulsive interactions, leading to an increase in the free volume (a decrease in the value of T_g). At relative high values of pH, most of the COOH groups in the PMAA segment would have dissociated into negatively charged COO^- groups; the resulting relatively rigid structures would also have the effect of increasing the value of T_g.

Fig. 10. Corresponding LCST behavior in photographs of the PNIPAm93-b-PMAA7 block copolymer in aqueous solution at various temperatures and values of pH.

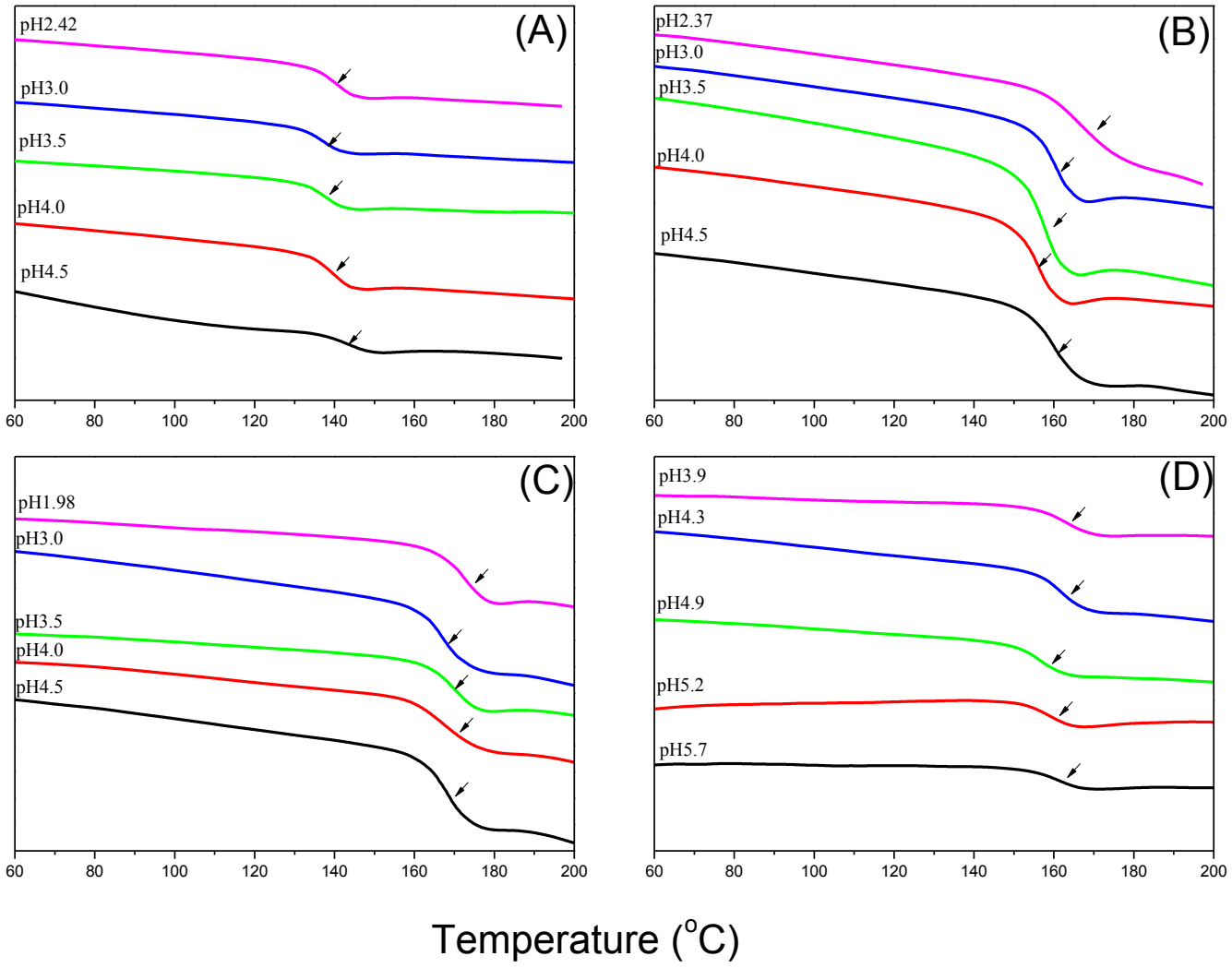

Fig. 11. DSC thermograms of (A) PNIPAm93-*co*-PMAA7, (B) PNIPAm79-*co*-PMAA21, and (C) PNIPAm74-*co*-PMAA26, and (D) the PNIPAm93-b-PMAA7 block copolymer cast from aqueous solutions at various values of pH.

Fig. 12 summarizes the DSC thermograms of thin films formed from the various PNIPAm-*co*-PMAA random and PNIPAm93-b-PMAA7 block copolymers after treatment at various values of pH and also after treatment under $scCO_2$ at 2000 psi and 32 °C for 1 h with subsequent depressurization for 1 h.

The values of T_g increased for PNIPAm-*co*-PMAA random copolymer, but the value of T_g decreased for the PNIPAm93-b-PMAA7 block copolymer, after $scCO_2$ treatment at the same value of pH. Kramer et al. proposed that the value of T_g may decrease because of the plasticizer effect when the hydrostatic pressure environment is not soluble in the polymer matrix. In contrast, the value of T_g may increase when the pressure environment is soluble in the polymer materials, thereby decreasing the free volume of the polymer matrix [45]. Because the CO_2 molecule can act as a Lewis acid and also can interact with the C═O units in the PNIPAm and PMAA segments through dipole–dipole interactions, it is possible that its presence increased the value of T_g for the PNIPAm-*co*-PMAA random copolymers, similar to the behavior observed in PNIPAm-*co*-PAA random copolymer systems [37]. In addition, the higher PMAA contents in the PNIPAm-*co*-PMAA random copolymers would lead to stronger dipole–dipole interactions with CO_2 and, therefore, higher values of T_g, as also displayed in Fig. 13.

For instance, CO_2 treatment at pH 3.5 caused the glass transition temperature of the PNIPAm93-*co*-PMAA7 random copolymer to increase only by 1 °C, whereas it increased by 3 °C for the PNIPAm74-*co*-PMAA26 random copolymer. As mentioned above, however, the PNIPAm93-b-PMAA7 block copolymer may form a micelle structure [Scheme 3(b)] with the PMAA block as the core and the PNIPAm block as the corona. Because CO_2 molecules can act as Lewis acids and interact better with the PMAA segment, they might stay in the core of the micelle structures after depressurization, due to hard evaporation at the core. As a result, it may exhibit a plasticizer effect and, thereby, decrease the value of T_g for the PNIPAm93-b-PMAA7 block copolymer.

Based on the significantly different phenomena exhibited by the various sequence length distributions of the PNIPAm-*co*-PMAA copolymers, we also investigated the CO_2-responsiveness of the PNIPAm93-b-PMAA7 block copolymer. Fig. 14 displays the behavior of the PNIPAm93-b-PMAA7 block copolymer in aqueous solution under the CO_2 bubbling (40 mL/h) at 75 °C; the pH decreased from

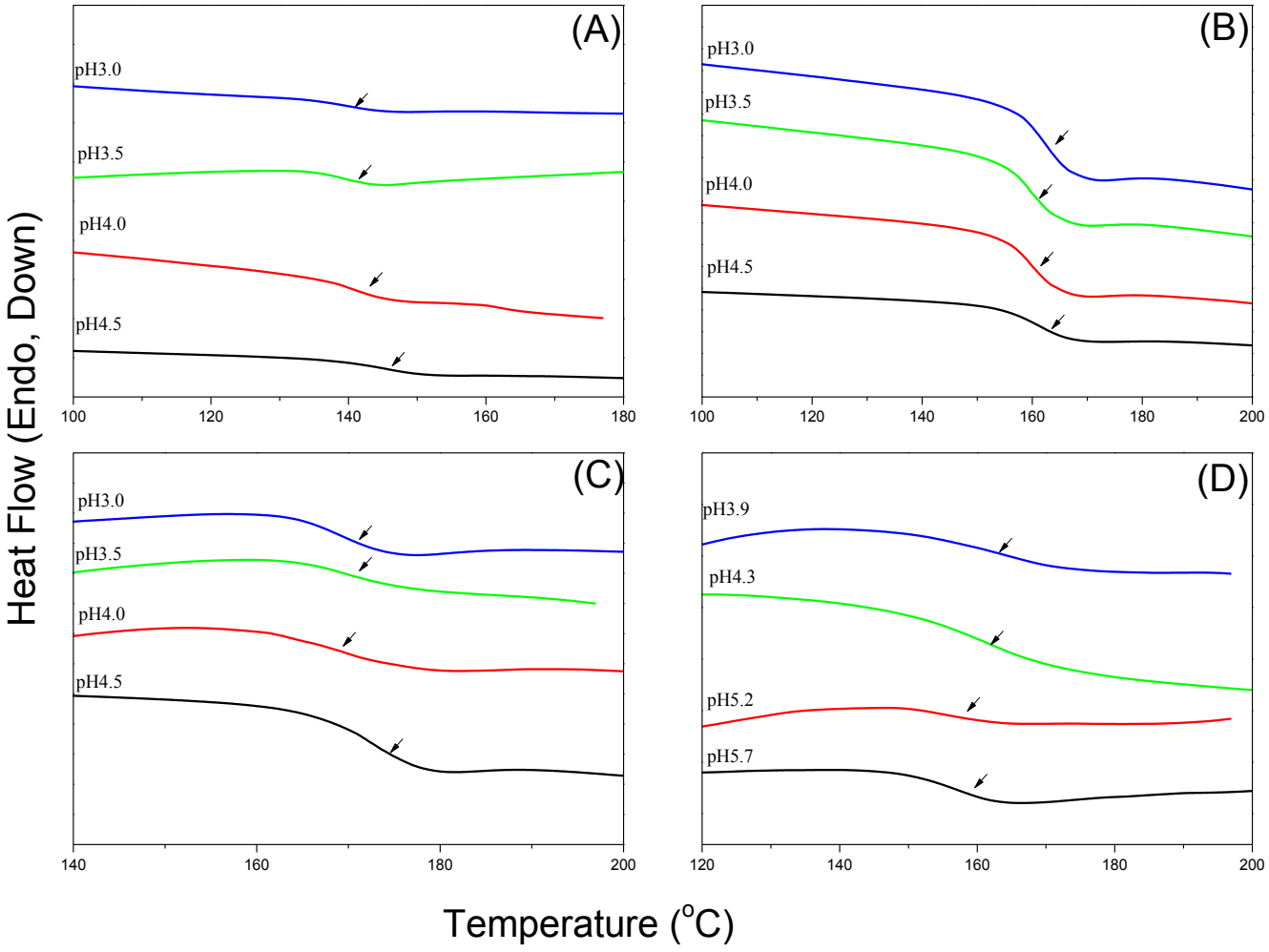

Fig. 12. DSC thermograms of films of (A) PNIPAm93-*co*-PMAA7, (B) PNIPAm79-*co*-PMAA21, and (C) PNIPAm74-*co*-PMAA26, and (D) the PNIPAm93-b-PMAA7 block copolymer, cast from aqueous solutions at various values of pH and after treatment in $scCO_2$ at 2000 psi and 32 °C for 1 h.

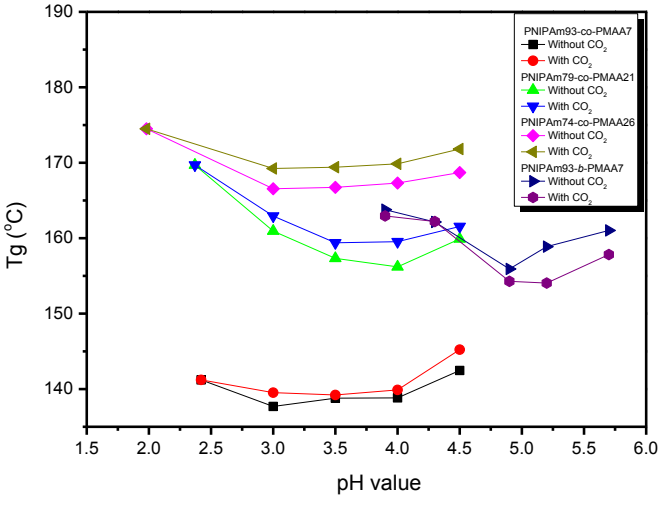

Fig. 13. Glass transition temperatures of films of the PNIPAm-*co*-PMAA random copolymers and PNIPAm93-*b*-PMAA7 block copolymer, cast from aqueous solutions at various values of pH, with or without $scCO_2$ treatment.

9.88 to 6.98 after 7 min because the CO_2 molecules acted as Lewis acids. Most importantly, the transparent aqueous solution formed an opaque aqueous solution after bubbling the CO_2, implying a change in the cloud point under these particular conditions. Furthermore, the opaque aqueous solution quickly (<1 min) reverted back to the transparent aqueous solution upon bubbling with N_2 (40 mL/h), due to the exchange of CO_2 with N_2, with an increase in the pH to 7.69, again indicating the change in the cloud point. This reversible phase behavior of the block copolymer could be repeated many times; no such behavior was observed for the random copolymers. Thus, the different sequence length effects of the PNIPAm-*co*-PMAA copolymers affected their physical properties dramatically, as has been widely discussed in our previous reports [19,20].

4. Conclusions

We have synthesized NIPAm/MAA random and block copolymers of various sequence length distributions through free radical copolymerizations and sequential RAFT polymerizations. Significant increases in glass transition temperatures occurred in both the random and block copolymers, due to strong hydrogen bonding between the carboxylic acid units of PMAA and the amide units of PNIPAm, as evidenced in FTIR and NMR spectroscopic analyses. The LCSTs increased upon increasing the pH for both the random and block copolymers because the COOH groups from the PMAA segment dissociated into COO^- groups, leading to greater

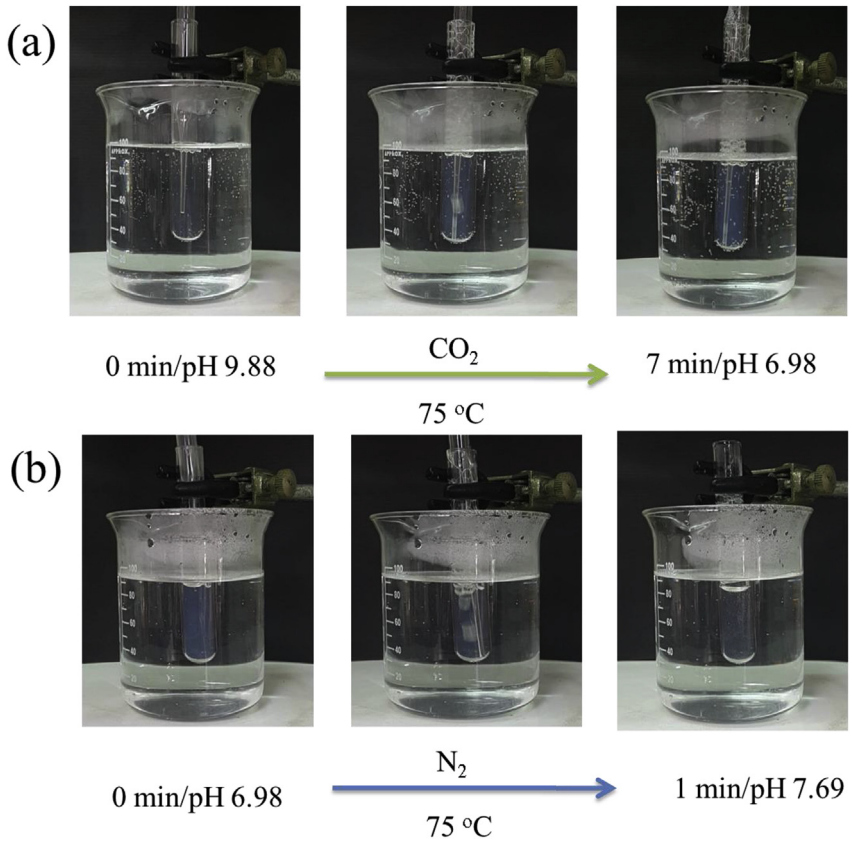

Fig. 14. Reversible phase transitions of the PNIPAm93-b-PMAA7 block copolymer under bubbling with (a) CO_2 and (b) N_2 at 75 °C.

solubility in aqueous solution. In addition, the LCST of the block copolymer varied significantly with respect to the pH, more so than that of the random copolymers, because of the sequence length distribution effect. The values of T_g for the random copolymers increased after treatment with $scCO_2$, but decreased after the similar treatment for the block copolymer. The block copolymer exhibited reversible CO_2-responsiveness in aqueous solution, as evidenced by the appearance and disappearance of cloudy aqueous solutions upon alternating the bubbling of CO_2 and N_2; this behavior was not observed for the random copolymers.

Acknowledgements

This study was supported financially by the Ministry of Science and Technology, Taiwan, under contracts MOST 105-2221-E-390-025-MY2 and by NSYSU-NUK Joint Research Project.

References

[1] S.W. Kuo, J. Polym. Res. 15 (2008) 459–486.
[2] M.M. Coleman, P.C. Painter, Prog. Polym. Sci. 20 (1995) 1–59.
[3] M. Jiang, L. Mei, M. Xiang, H. Zhou, Adv. Polym. Sci. 146 (1999) 121–196.
[4] Y. He, B. Zhu, Y. Inoue, Prog. Polym. Sci. 29 (2004) 1021–1051.
[5] S.W. Kuo, F.C. Chang, Macromolecules 34 (2001) 5224–5228.
[6] Z. Yang, C.D. Han, Macromolecules 41 (2008) 2104–2118.
[7] K.A. Masser, J. Runt, Macromolecules 43 (2010) 6414–6421.
[8] C.F. Wang, Y.C. Su, S.W. Kuo, C.F. Huang, Y.C. Sheen, F.C. Chang, Angew. Chem. Int. Ed. 45 (2006) 2248–2251.
[9] K. Dobrosielska, S. Wakao, A. Takano, Y. Matsushita, Macromolecules 41 (2008) 7695–7698.
[10] T.S. Tsai, Y.C. Lin, E.L. Lin, Y.W. Chiang, S.W. Kuo, Polym. Chem. 7 (2016) 2395–2409.
[11] H. Miyase, Y. Asai, A. Takano, Y. Matsushita, Macromolecules 50 (2017) 979–986.
[12] J. Kwak, S.H. Han, H.C. Moon, J.K. Kim, Macromolecules 48 (2015) 6347–6352.
[13] H. Xu, S. Srivastave, V.M. Rotello, Adv. Polym. Sci. 207 (2007) 179–198.
[14] S.W. Kuo, F.C. Chang, Prog. Polym. Sci. 36 (2011) 1649–1696.
[15] C.W. Chiou, Y.C. Lin, L. Wang, R. Maeda, T. Hayakawa, S.W. Kuo, Macromolecules 47 (2014) 8709–8721.
[16] S.W. Kuo, S.C. Chan, F.C. Chang, Macromolecules 36 (2003) 6653–6661.
[17] M.M. Coleman, P.C. Painter, Miscible Polymer Blends: Background and Guide for Calculations and Design, DEStech Publication Inc, Lancaster, PA, 2006.
[18] S.W. Kuo, C.T. Lin, J.K. Chen, F.H. Ko, F.C. Chang, Polymer 52 (2011) 2600–2608.
[19] S.W. Kuo, P.H. Tung, F.C. Chang, Macromolecules 39 (2006) 9388–9395.
[20] C.L. Lin, W.C. Chen, C.S. Liao, Y.C. Su, C.F. Huang, S.W. Kuo, F.C. Chang, Macromolecules 38 (2005) 6435–6444.
[21] M.M. Coleman, Y. Xu, P.C. Painter, Macromolecules 27 (1994) 127–134.
[22] S.W. Kuo, H. Xu, C.F. Huang, F.C. Chang, J. Polym. Sci., Part B: Polym. Phys. 40 (2002) 2313–2323.
[23] J.E. Stumpel, E.R. Gil, A.B. Spoelstra, C.W.M. Bastiaansen, D.J. Broer, A.P.H. Schenning, Adv. Funct. Mater. 25 (2015) 3314–3320.
[24] M. Cheng, Q. Liu, G. Ju, Y. Zhang, L. Jiang, F. Shi, Adv. Mater. 26 (2014) 306–310.
[25] H.G. Schild, Prog. Polym. Sci. 17 (1992) 163–249.
[26] H. Cheng, L. Shen, C. Wu, Macromolecules 39 (2006) 2325–2329.
[27] D. Schmaljohann, Adv. Drug Deliv. Rev. 58 (2006) 1655–1670.
[28] X. Qiu, C.M.S. Kwan, C. Wu, Macromolecules 30 (1997) 6090–6094.
[29] M. Shibayama, Y. Fujikawa, S. Nomura, Macromolecules 29 (1996) 6535–6540.
[30] J. Zhuang, M.R. Gordon, J. Ventura, L. Li, S. Thayumanavan, Chem. Soc. Rev. 42 (2013) 7421–7435.
[31] S.G. Kazarian, M.F. Vincent, F.V. Bright, C.L. Liotta, J. Am. Chem. Soc. 118 (1996) 1729–1736.
[32] Y.T. Shieh, K.H. Liu, J. Supercrit. Fluids 25 (2003) 261–268.
[33] Y.T. Shieh, T.Y. Zhou, S.W. Kuo, RSC Adv. 6 (2016) 75032–75037.
[34] J. Zhang, L.Y. Chu, Y.K. Li, Y.M. Lee, Polymer 48 (2007) 1718–1728.
[35] K.C. Clarke, S.N. Dunham, L.A. Lyon, Chem. Mater. 27 (2015) 1391–1396.
[36] F. Leonforte, M. Muller, Macromolecules 49 (2016) 5256–5265.
[37] Y.T. Shieh, P.Y. Lin, S.W. Kuo, Polymers 8 (2016) 434.
[38] H.K. Fu, S.W. Kuo, C.F. Huang, F.C. Chang, H.C. Lin, Polymer 50 (2009) 1246–1250.
[39] S.W. Kuo, F.C. Chang, Polymer 42 (2001) 9843–9848.
[40] S.W. Kuo, R.S. Cheng, Polymer 50 (2009) 177–188.

[41] T.K. Kwei, J. Polym. Sci. Polym. Lett. Ed. 22 (1984) 307–313.
[42] G. Chen, A.S. Hoffman, Nature 373 (1995) 49–52.
[43] C. Boutris, E.G. Chatzi, C. Kiparissides, Polymer 38 (1997) 2567–2570.
[44] J.N. Zhang, A. Peppas, Macromolecules 33 (2000) 102–107.
[45] W.C. Wang, E.J. Kramer, J. Polym. Sci. Polym. Phys. Ed 20 (1982) 1371–1384.